



# Influence of building heat distribution temperatures on the energy performance and sizing of 5th generation district heating and cooling networks

Alessandro Maccarini<sup>a,\*</sup>, Artem Sotnikov<sup>b</sup>, Tobias Sommer<sup>b</sup>, Michael Wetter<sup>c</sup>, Matthias Sulzer<sup>d</sup>, Alireza Afshari<sup>a</sup>

<sup>a</sup> Department of the Built Environment, Aalborg University, A.C. Meyers Vænge 15, 2450, Copenhagen, Denmark

<sup>b</sup> Institute of Building Technology and Energy, Lucerne University of Applied Sciences and Arts, CH 6048 Horw, Switzerland

<sup>c</sup> Building Technology and Urban Systems Division, Lawrence Berkeley National Laboratory, 1 Cyclotron Road, Berkeley, CA, 94720, USA

<sup>d</sup> Empa, Swiss Federal Laboratories for Materials Science and Technology, CH 8600, Dübendorf, Switzerland

## ARTICLE INFO

Handling Editor: Henrik Lund

### Keywords:

District heating  
District cooling  
5GDHC  
Heat Pumps  
Modelica  
Building heating systems

## ABSTRACT

This paper investigates the energy performance and sizing criteria of 5th generation district heating and cooling (5GDHC) networks as a function of the heat distribution temperature in the building systems connected to the district network. An energy simulation model of a 5GDHC network was developed in Modelica for a case study located in Denmark. Calculations were carried out for four different building heating systems. Simulation results show that reducing the heat distribution temperatures from 70 °C to 23 °C leads to around 40% annual electric energy savings (from 10.4 kWh/m<sup>2</sup> to 6.2 kWh/m<sup>2</sup>) for the operation of the heat pumps. Heat distribution temperatures of 23 °C cause higher water mass flow rates through the network, leading to annual electric energy consumption for the circulation pumps that are almost doubled (from 0.16 kWh/m<sup>2</sup> to 0.3 kWh/m<sup>2</sup>) compared to the reference case at 70 °C. Furthermore, the paper discusses how the results obtained from the Danish case study can be generalized and applied to other cases using a simplified mathematical approach. It is found that about 1.5% of electric energy savings can be achieved for each temperature degree reduction in the heat distribution system.

## 1. Introduction

### 1.1. Background

Today, 55% of the world's population lives in urban areas, a proportion that is expected to increase to 68% by 2050 [1]. Urbanization is a challenge that combines social, economic, and environmental issues. From an energy point of view, it offers the opportunity to implement infrastructures that can contribute to the reduction of CO<sub>2</sub> emissions. In this context, district heating and cooling systems are expected to play an important role towards the decarbonization of cities and communities.

The concept of district heating (DH) was developed by means of centralized production of heat and its distribution to final users by a network of pipes. Historically, four generations of DH are recognized [2]. The so-called 1st generation of district heating networks was introduced in the late 1800s century using steam as a heat carrier. These

systems were replaced by 2nd generation networks, which use pressurized liquid water instead of steam, with supply temperatures over 100 °C. The 3rd generation (3GDH) of systems was introduced in the 1970s and it is characterized by supply water temperatures often below 100 °C. The so-called 4th generation of district heating (4GDH) networks is a recent district heating concept, and it is identified by even lower temperature levels (30–70 °C) and the integration of renewable energy sources.

Case studies show that the transition from 3GDH to 4GDH is cost and energy effective. For example, the case of Aalborg municipality revealed that moving from 3GDH to 4GDH decreased the primary energy consumption of the energy system by around 4.5% and the costs of the system by 2.7% [3]. Averfalk et al. [4] reported higher profitability of 4GDH in comparison to 3GDH for a case study located in the city of Strasbourg.

Despite the improvements achieved by 4GDH networks in terms of

\* Corresponding author.

E-mail address: [amac@build.aau.dk](mailto:amac@build.aau.dk) (A. Maccarini).

<https://doi.org/10.1016/j.energy.2023.127457>

Received 19 September 2022; Received in revised form 16 February 2023; Accepted 5 April 2023

Available online 13 April 2023

0360-5442/© 2023 Published by Elsevier Ltd.

energy efficiency, integration of renewable sources and cost, the topology of 4GDH systems is often identical to that of the previous generations: the network of pipes is designed to deliver exclusively thermal energy for heating to connected users. This can be seen as a limitation, especially considering two aspects. First, urban areas typically consist of a mix of residential, commercial, and industrial buildings that require simultaneous heating and cooling. Second, energy demand for space cooling has grown rapidly since the 1990s [5], and this trend is expected to continue in the future due to global warming, building thermal insulation and raising comfort standards. For these reasons, current research focuses on new thermal networks that can deliver both heating and cooling services using the same pipes. Such networks are often defined as the 5th generation of district heating and cooling (5GDHC) networks [6–8]. It is acknowledged that the label 5GDHC has caused some divergence within literature [9,10], and other terms have been coined to define such DHC networks, namely: i) *Cold district heating* [11], ii) *Bidirectional low-temperature networks* [12], iii) *Anergy networks* [13], iv) *Neutral Temperature District Heating* [14]. In this study, they are referred to as 5GDHC networks.

In 5GDHC networks, distribution water temperature is close to ground temperature (approximately between 5 and 35 °C [15]), and therefore, not suitable for direct heating. Buildings are equipped with substations consisting of water source heat pumps (HPs), which can lift temperatures to those required by the user for space heating and domestic hot water. Cooling can either be provided passively with heat exchangers, or actively with chillers, supplying their waste heat back into the network. One of the advantages of using decentralized HPs is related to the possibility of supplying heat at temperatures adapted for each end-user. In comparison, centralized traditional district networks are constrained by the worst end-user's temperature level. Other advantages of 5GDHC networks are the reduction of heat losses in the distribution network and the direct exploitation of low-temperature heat sources. On the other hand, more complex and expensive substations compared to traditional systems are necessary. Moreover, due to the small temperature difference between supply and return pipes (or warm and cold pipes), higher volumetric flow rates are required to provide the same thermal power with respect to a traditional DH network. To limit pressure losses, pipes with large diameters are typically installed. However, as these systems operate with near ground temperatures, they are generally non-insulated.

### 1.2. Previous work on 5GDHC systems

Despite the concept of 5GDHC being relatively new, several systems are in operation in Europe [6]. Most of them were constructed as pilot or demonstration projects [16–19], and operational performance and monitoring data are seldom available. Thus, the experience gained from such projects is often limited, and this makes it challenging to develop the 5GDHC concept for implementation in large urban areas consisting of hundreds or thousands of buildings. To fill this gap, in recent years, most of the research studies have focused on the development of numerical models capable of carrying out preliminary design, equipment sizing and energy performance analysis of 5GDHC networks.

Wirtz et al. [20] presented a novel methodology based on linear programming for designing and evaluating bidirectional 5GDHC systems. When applied to a real-world use case in Germany, this design approach showed a cost reduction of 42% and caused 56% less CO<sub>2</sub> emissions compared to individual heating, ventilation, and air conditioning (HVAC) systems.

Zarin Pass et al. [21] explored the environmental benefits of 5GDHC systems by means of exergy efficiency. A diversity metric was developed to understand in which cases bidirectional DHC networks may be more efficient than individual-building systems. This metric was then applied to reference building load profiles in three cities. It was found that a bidirectional system has benefits when the ratio of heating to cooling loads on average is at least 1 to 5.7 or vice versa.

Wetter and Hu [22] analyzed the controllability of bidirectional networks in which each substation draws water from a warm distribution pipe and feeds it back to a colder distribution pipe if in heating mode, and vice versa if in cooling mode. They concluded that such bidirectional networks are hard to control as substations can induce in other substations instabilities that are propagated to the whole system via the water pressure fluctuations. They therefore proposed to use a so-called reservoir network, a novel 5GDHC system topology based on [23]. The reservoir network uses a one-pipe hydraulic circuit where substations are connected in series. Sommer et al. [24] further optimized the reservoir network. Results from dynamic simulations show that, if the network is operated with variable mass flow rate, total electric energy consumption differs by less than 1% between the reservoir and the bidirectional system.

Von Rhein et al. [25] developed a software tool to analyze the feasibility of 5GDHC systems in both new and existing districts. The tool is able to identify the optimal network layout and it can calculate the performance of the network based on various output metrics, including primary energy usage, CO<sub>2</sub> emissions, and network implementation cost. Another software tool to optimize district energy systems was developed by Wirtz [26]. The tool is intended for early planning phases, and it helps to generate tailor-made profiles for heating, cooling, and electricity demands. In addition, the tool implements models for DHC networks (including 5GDHC).

Wirtz et al. [27] proposed a mixed-integer linear program (MILP) for short-term optimization of the network temperature in 5GDHC systems. In a case study, this optimization approach leads to cost savings in two of the three investigated months (by 10% and 60% respectively) compared to a reference operation strategy based on free-floating temperature. This paper also shows that controlling the network temperature in summer to enable direct cooling (by heat exchangers instead of chillers) is of great importance for the overall network efficiency.

Bünning et al. [12] developed a control concept based on a temperature set point optimization and agent-based control which allows the modular integration of an arbitrary number of sources and consumers in 5GDHC systems. The concept was applied to two locations (San Francisco and Cologne) representing neighbourhoods with different heating and cooling demands and boundary conditions. For both locations, the bidirectional network with agent-based control was the most efficient technology. In comparison to a conventional gas-fired district heating system, the optimized network leads to primary energy consumption reductions of 58% and 84% in the US and German scenario, respectively. Reductions in CO<sub>2</sub> emissions are 35% and 78%, and reductions in energy costs are 53% and 57%.

Sommer et al. [28] summarize hydrothermal challenges in 5GDHC, focussing on operational dynamics such as interaction of substations and their effect on flow rate and temperature limitations of heat pumps. They collect various criteria in a decision-making matrix and point out that, in particular in 5GDHC systems, network choice should take into account operational aspects in addition to quantifiable parameters such as costs or emissions. For one case study, they investigate network efficiency based on flow rate through the network.

Edtmayer et al. [29] investigated how the heat energy production through industrial heat pumps and the total thermal capacities of 5GDHC networks can provide flexibility for power to heat applications. The authors simulated a district network of 2200 houses and evaluated the flexibility offered to the grid with response to thermal comfort (internal temperature between 20 and 24 °C).

Abugabbara et al. [30] developed a simulation model for the design and analysis of 5GDHC systems. The model was employed to simulate the first existing Swedish DHC system with bidirectional energy flows. Results revealed several benefits for integrating district and heat pump technologies, including sharing energy flows between interconnected buildings, reducing the total purchased energy, and reducing distribution losses.

Quirosa et al. [31] studied the integration of 5GDHC systems with



Fig. 1. Layout of the urban area of Køge Nord.

photovoltaic generation installed in the buildings to improve flexibility by coupling thermal and electric sectors. Such integration led to about 30% reduction of grid electricity consumption.

### 1.3. Novel contributions

As mentioned in section 1.1, the major interest in using decentralized heat pumps is to supply heat at temperature levels adapted to each end-user. This is a particular advantage in areas populated with buildings having different temperatures of heat distribution. This also means that the overall energy performance (i.e., electricity consumption) of 5GDHC networks strictly depends on the typology of heat distribution systems installed in the buildings connected to the district heating systems.

Research analyzing building heating systems with different heat distribution temperatures have been reported in literature. Gonçalves et al. [32] performed a comparative energy and exergy analysis of eight space heating options. Different emission systems with heat distribution temperatures varying between 70 °C and 40 °C were considered in combination with different plants and heat generators. A similar study was performed by Kazanci et al. [33], who carried out an exergy comparison of three space heating systems under different operating conditions. When considering the combination of floor heating with air-source heat pump, results indicated that 14% higher exergy input is required when increasing the supply water temperature from 33 °C to about 40 °C. Kerdan et al. [34] developed an exergy-based multi-objective optimization tool to assess the impact of a diverse range of retrofits measures, including HVAC configurations. For a school building model connected to a ground source heat pump, an exergy destruction reduction of 40% was achieved by replacing fan coil units with under-floor heating.

It appears that previous works on this topic focused only on building level, where different heat distribution systems are described and compared using a single building as case study. However, no study has

**Table 1**  
Overview of building typologies.

Typology	N. units	Floor area (per unit) [m <sup>2</sup> ]	Total floor area [m <sup>2</sup> ]
Terraced house (TH)	153	96	14,688
Multi-family house (MFH)	50	242	12,100
Block apartment (BA)	73	800	58,400
Office (OF)	5	10,000	50,000

quantified the influence of building heat distribution temperatures at district level in the context of 5GDHC systems. Such investigation is critical as the efficiency of decentralized heat pumps, which is mainly influenced by the temperature lift, has a direct impact on the sizing and operation of the water distribution in the district piping network and its overall energy performance.

To fill the existing research gap, this paper presents a 5GDHC energy simulation model, whose energy performance is calculated for different heat distribution systems in the buildings. Simulations are carried out for a case study located in Denmark. The paper also discusses how the results obtained from the Danish case study can be generalized and applied to other cases using a simplified mathematical approach.

### 1.4. Paper organization

The paper is structured as follows: Section 2 describes the case study and the energy simulation models adopted; Section 3 presents the simulation results obtained by comparing the four different building heating systems; Section 4 illustrates the limitations of this study; Section 5 discusses the results in terms of pipe sizing and generalizability; and Section 6 concludes the article by summarizing the findings.

## 2. Methodology

This section introduces the urban area of Køge Nord, which was considered as a case study, and then describes the numerical models used for the analysis.

### 2.1. Urban area and network topology

#### 2.1.1. Demand profiles

Køge Nord is a newly planned urban development area located in Køge, a municipality in Denmark with a population of approximately 62,000 and an area of about 260 km<sup>2</sup> [35]. The portion of the urban area considered in this use case will be developed around the Køge Nord train station (55°29'58"N 12°10'19"E) and it consists of a mix of residential and commercial buildings, as illustrated in Fig. 1. Table 1 provides an overview of the amount and typologies of building units included in the analysis. Detailed geometries of the building typologies are illustrated in Fig. 2.

Hourly demand profiles for space heating, domestic hot water, and space cooling, were calculated using the tool BAGEL [36]. This Python-based tool enables users to create simplified building geometries, assign input parameters (e.g., U-values, ventilation rates, internal gains), execute energy simulations and output hourly profiles of heating and cooling loads. To execute simulations, BAGEL uses a resistance-capacitance building model, as specified in the ISO 13790 standard [37]. This model describes the thermo-physical behaviour of buildings by means of an equivalent electric circuit consisting of five resistances and one capacity (5R1C). Such a reduced-order model was used in this work due to its ability to combine good accuracy with low computation and parameterization requirements.

Table 2 shows the input parameters used for simulations for each building typology. Since this is a newly planned urban area, not all information was available about the characteristics of the buildings.

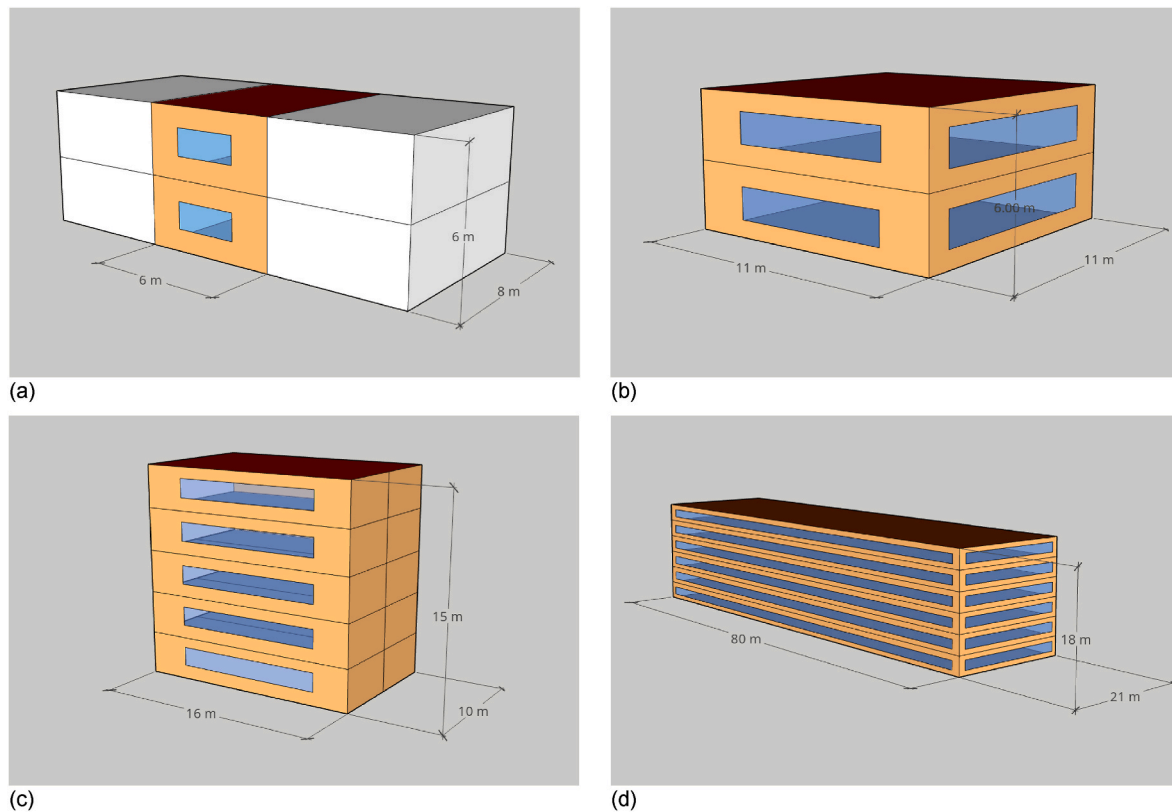


Fig. 2. Geometries of building typologies: terraced house (a), multi-family house (b), block apartments (c), and office (d).

Table 2  
Input parameters for building energy models.

Parameter	Residential (TH, MFH, BA)	Offices
U-value walls (W/m <sup>2</sup> K)	0.3	0.3
U-value Roof (W/m <sup>2</sup> K)	0.2	0.2
U-value Floor (W/m <sup>2</sup> K)	0.2	0.2
U-value Window (W/m <sup>2</sup> K)	1.1	1.1
Window-to-wall ratio	0.25	0.4
G-factor window	0.5	0.5
Ventilation rate (ACH)	0.4	1.25
Effectiveness of heat recovery unit	0.8	0.8
Natural cooling ventilation rate (ACH)	–	Up to 6
Internal heat gains (W/m <sup>2</sup> )	5 (weekly schedule)	25 (weekly schedule)
DHW (W/m <sup>2</sup> )	1.5 (constant)	0.6 (constant)
Heating set-point (°C)	20	21
Cooling set-point (°C)	–	24

Therefore, most of the input parameters were selected according to architectural master plan, Danish building regulations and authors' assumptions. Cooling demand was considered only for offices as cooling systems are not typically installed in Danish residential buildings. In office buildings, a natural cooling control strategy was adopted, allowing high outdoor air flow rates to enter the building when favourable outdoor conditions occur. Weather data of Copenhagen (Denmark) were used for simulations. Fig. 3 shows the annual outdoor air temperature distribution [38].

Fig. 4 shows the hourly demand profiles of the urban area. The annual heating demand (space heating plus domestic hot water) of the residential buildings is 2.72 GWh/y, which corresponds to a specific heating demand of 28.6 kWh/m<sup>2</sup>y. The annual heating and cooling

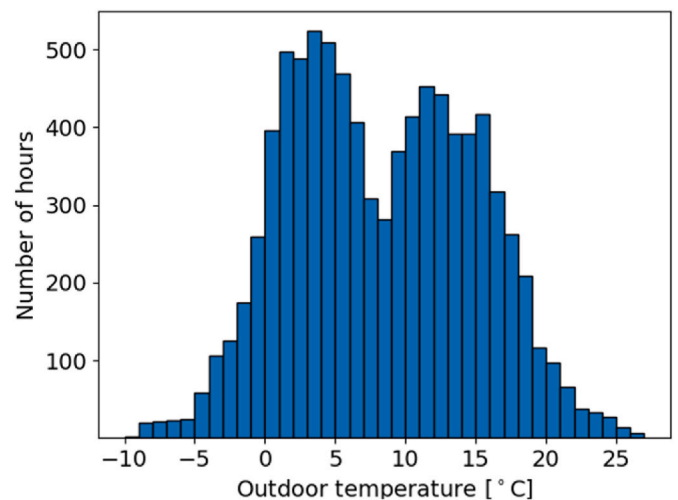


Fig. 3. Annual outdoor air temperature distribution for Copenhagen climate.

demands of the office buildings are 1.34 GWh/y and 0.3 GWh/y, respectively, which correspond to 26.8 kWh/m<sup>2</sup> of specific heating demand and 6 kWh/m<sup>2</sup> of specific cooling demand. Globally, the urban area has a heating demand of 4.06 GWh/y and a cooling demand of 0.3 GWh/y. The overall ratio of heating to cooling demand is about 14.

### 2.1.2. Network topology

Fig. 5 illustrates the layout of the 5GDHC network considered in this work. According to a classification of district thermal networks provided by Refs. [6,39], this network topology is characterized by *bidirectional energy flow* and *directional fluid flow*. The term *bidirectional energy flow*

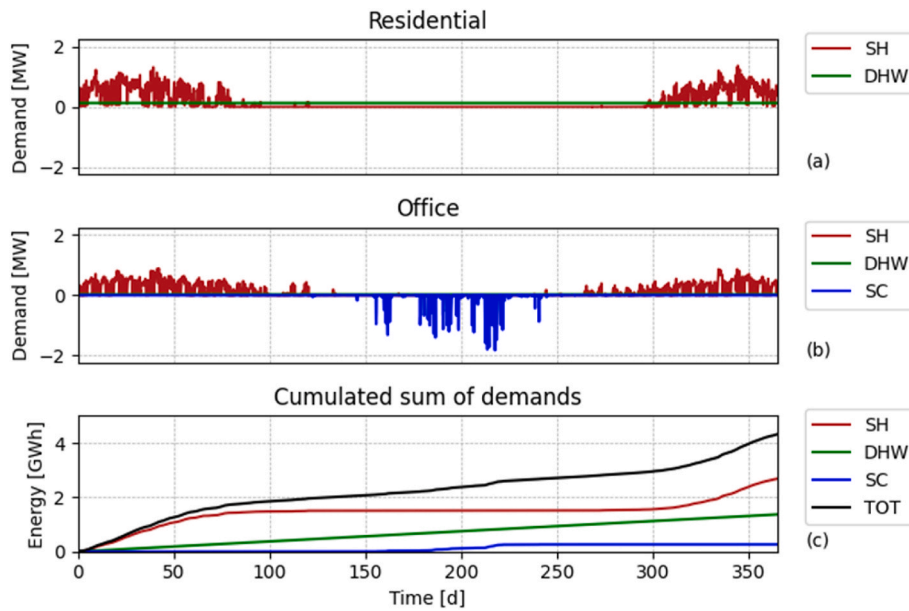


Fig. 4. Demand profiles of the residential area (a), office area (b) and cumulative sum of demands for the entire urban area (c). The legend indicates demand for space heating (SH), domestic hot water (DHW), space cooling (SC) and total (TOT).

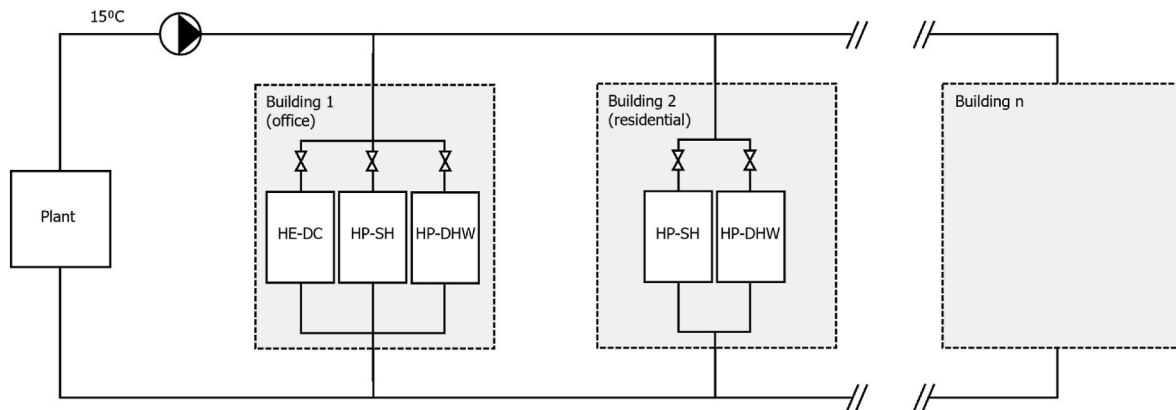


Fig. 5. Layout of the 5GDHC system. Substations for office buildings consist of a heat pump for space heating (HP-SH), a heat pump for domestic hot water (HP-DHW) and a heat exchanger for direct cooling (HE-DC). Substations of residential buildings do not integrate the HE-DC, as no cooling is considered.

refers to the fact that the network can deliver both heating and cooling simultaneously. This is due to the use of a supply water temperature of 15 °C. The term *directional fluid flow* means that the fluid direction in the network is predefined using a centralized circulation pump.

The central plant consists of a limitless renewable source at 15 °C, which can keep the supply water temperature in the network constant. Such a renewable source can be, for example, a lake, ground water, sewage water, or wastewater from industries or data centres.

The substations of office buildings consist of three main components: a heat pump for space heating, a heat pump for domestic hot water and a heat exchanger for direct cooling. As cooling of residential buildings was not considered, the substations of residential buildings integrate only the two heat pumps.

## 2.2. Heat distribution temperatures in buildings

To investigate the influence of heat distribution temperatures on the energy performance of the 5GDHC network, four different cases were analyzed, namely high-temperature radiator (HT-R), mid-temperature radiator (MT-R), low-temperature floor heating (LT-F) and room-temperature beam (RT-B). Table 3 illustrates the design heat

Table 3

Heat distribution temperatures for the four cases (design conditions).

Case	Heat distribution temperature at -10 °C
High-temperature radiator (HT-R)	70 °C
Mid-temperature radiator (MT-R)	55 °C
Low-temperature floor heating (LT-F)	35 °C
Room-temperature beam (RT-B)	23 °C

distribution temperatures assumed for each case. Note that the heat distribution temperature corresponds to the temperature of the water leaving the heat pump condenser, which is the water temperature delivered to the building. The heat distribution temperatures are reset based on the outdoor air temperature, as shown in Fig. 6.

The case RT-B refers to a novel HVAC system that integrates active beams to provide heating with water distribution temperatures at 23 °C. The technical feasibility of such a system has been previously demonstrated through energy simulation analyses [40,41] and on-site monitoring [42]. Even though the applicability of the RT-B system has been tested only for office buildings, in this study, it is assumed that such a system could be installed also in residential buildings.

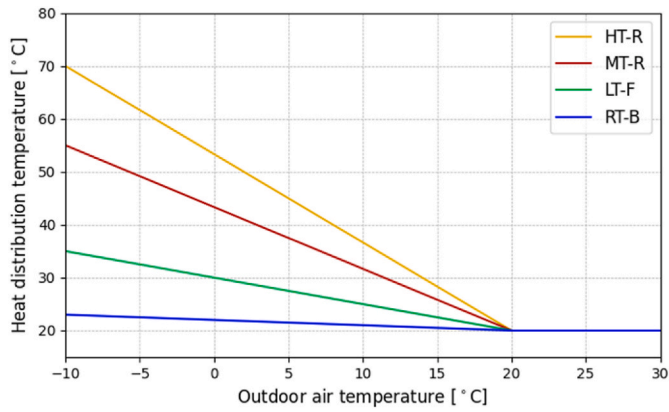


Fig. 6. Heat distribution temperatures reset based on the outdoor air temperature.

2.3. Detailed dynamic model

The detailed dynamic model of the 5GDHC network was developed using the Modelica language, and it describes the thermal and hydraulic dynamics of the network. Modelica is a freely available, object-oriented and equation-based language for modeling physical systems and controls [43], and it has already been successfully applied in the dynamic modeling of district thermal networks [12,24,44–46]. Component models from the Modelica Buildings Library version 8.0.0 [47] were used in this work. Simulations were run using Dymola 2022 on Windows with the DASSL solver and a tolerance of 1E-6. All simulations were run for a one-year period. Fig. 7 illustrates the Modelica diagram view of the district network.

To reduce the modeling and simulation effort, the 281 building units were aggregated into 5 building clusters. Fig. 8 shows the spatial distribution of the building clusters, together with the piping route and the annual heating and cooling energy demand.

The next few sections describe the physical assumptions made for the main component models.

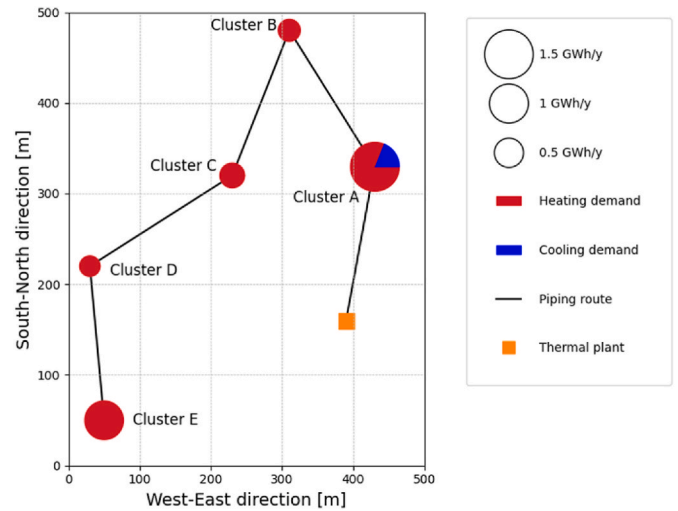


Fig. 8. Spatial distribution of building clusters.

2.3.1. Heat pumps and heat exchanger for cooling

Heat pumps were modelled using the model *Carnot\_TCon*. This model tracks the set point of the water temperature leaving the condenser (heat distribution temperature) using an idealized internal control. The COP of the heat pump model is computed as

$$COP = \eta \frac{T_{con}}{T_{con} - T_{eva}}, \tag{1}$$

where  $\eta = 0.4$  is the Carnot effectiveness of the heat pump construction,  $T_{con}$  is the condenser temperature and  $T_{eva}$  is the evaporator temperature. To avoid violating the second law of thermodynamics, the model assumes the evaporator and condenser temperatures to be equal to the water outlet temperatures. Pinch temperatures of 2 K at design conditions were considered in this model to account for temperature difference between refrigeration and working fluid. For off-design conditions, these pinch temperatures are scaled proportionally to the ratio of actual

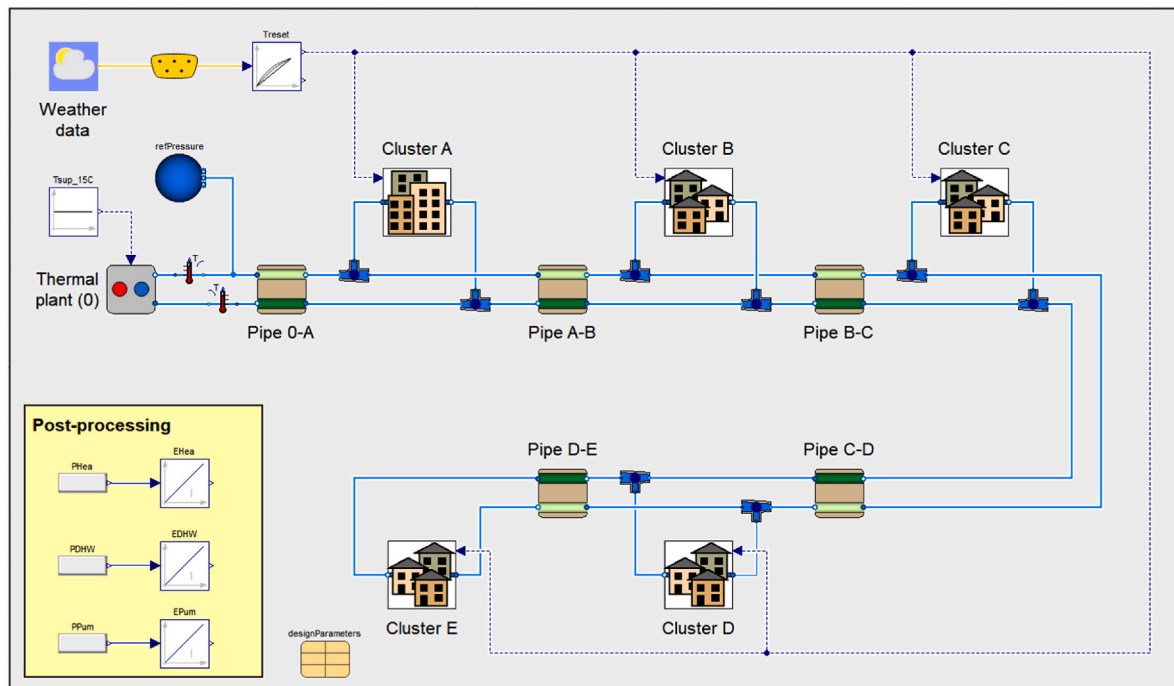


Fig. 7. Modelica diagram view of the district network.

heat flow rate at the condenser (or evaporator) divided by the nominal heat flow rate at the condenser (or evaporator). Based on the input hourly demand profile and the calculated COP, the model computes the water mass flow rate that needs to be drawn from the district network to satisfy a temperature difference of 4 K of the working fluid (design assumption).

Space cooling is provided using a heat exchanger that calculates the required water flow rate from the network in the amount of

$$\dot{m} = \frac{\dot{Q}_{sc}}{c_p \Delta T}, \quad (2)$$

Where  $\dot{Q}_{sc}$  is the space cooling demand,  $c_p$  is the specific heat capacity of water and  $\Delta T$  is the temperature difference on the network side (4 K). The cooling system operates with supply water temperatures of 20 °C (building side). A pressure drop of 50 kPa at design flow rate was assumed in both heat pumps and heat exchangers.

### 2.3.2. Plant

The plant was modelled using the model *PrescribedOutlet*. This model sets the temperature of the outlet water to a given value. In this case, an outlet set-point temperature of 15 °C was assumed. Therefore, the plant is considered as an unlimited source of energy at 15 °C, which can cover the entire heating and cooling demands imposed by the network. A pressure drop of 50 kPa at design flow rate was assumed in the plant.

### 2.3.3. Network pipes

The network piping was modelled using the model *PressureDrop*. This model computes the flow resistance using a fixed flow coefficient which is calculated based on a user-defined pressure drop at a user-defined design flow rate. For lower flow rates, e.g. during summer operation, these values are reduced, as the simulation model computes flow friction as a function of the flow rate.

The sizing of network pipes was carried out by assuming a pressure drop per pipe length of 200 Pa/m at design mass flow rate. The design mass flow rate of each pipe segment was calculated as the required mass flow rate to satisfy the respective peak heating (or cooling) load with a temperature difference of 4 K between inlet and outlet, assuming a default COP of 3. This value was selected only for sizing purposes, and it corresponds to a generic heating system with distribution temperatures of 55 °C. The resulting pipe diameters varied between 0.13 m and 0.24 m within the network.

### 2.3.4. Ground model

The heat transfer between the water in the pipes and the ground was modelled as shown in Fig. 9. This model represents a radial, one-dimensional discretization of the transient heat conduction equation:

$$\rho c \left( \frac{\partial T}{\partial t} \right) = k \left( \frac{\partial^2 T}{\partial r^2} + \frac{1}{r} \frac{\partial T}{\partial r} \right), \quad (3)$$

where  $\rho = 540 \text{ kg/m}^3$  is the density,  $c = 1210 \text{ J/kg K}$  is the specific heat capacity,  $k = 2.8 \text{ W/mK}$  is the heat conductivity, and  $T$  is the temperature at location  $r$  and time  $t$  and. To spatially discretize the heat equation, the ground was divided into compartments (finite volumes), consisting of thermal capacitances connected through thermal resistances.

The undisturbed ground temperature boundary condition  $T_g$  was set at 0.5 m distance from the pipe, and its value was pre-calculated according to a formula as a function of the time of the year and the depth below the ground surface [48]. The yearly profile of  $T_g$  is illustrated in Fig. 10a. The pipes were uninsulated and located at 1 m underground. Heat exchange between supply and return pipes was ignored.

### 2.3.5. Circulation pump

The purpose of the central pumping unit is to ensure the necessary

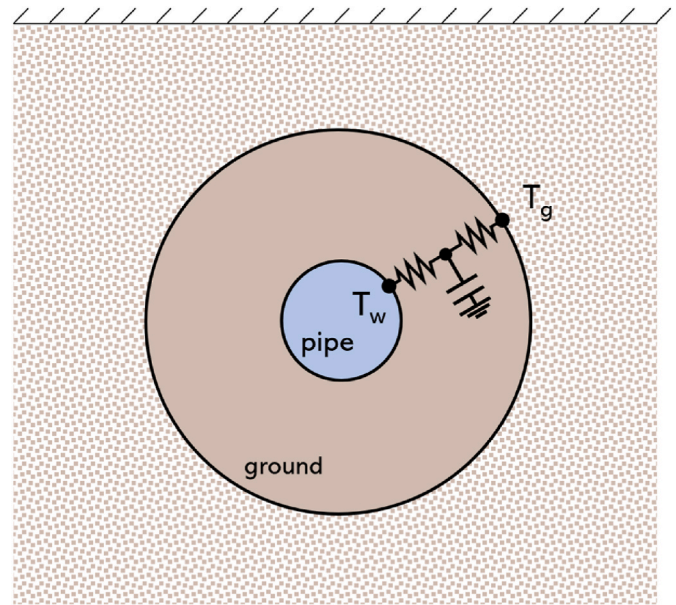


Fig. 9. Ground model.

water flow in the network. The circulation pump was modelled using the model *FlowControlled\_m\_flow*. This model is capable of providing the required mass flow rate at any time by overcoming the corresponding pressure loss. The electric power required is determined by the hydraulic efficiency and the motor efficiency and it is computed as

$$P_{ele} = \frac{V \Delta p}{\eta_{mot} \eta_{hyd}}, \quad (4)$$

where  $V$  is the volumetric flow rate,  $\Delta p$  is the pressure drop,  $\eta_{mot}$  is the motor efficiency and  $\eta_{hyd}$  is the hydraulic efficiency. A constant value of 0.7 was assumed for both the motor efficiency and the hydraulic efficiency. Note that to simplify the modeling and simulation, the central circulation pump was represented by decentralized pumps in each substation, which replace valves. This modeling simplification has a negligible effect on the simulation results investigated in this article.

## 3. Results

### 3.1. Network water temperatures, flow rates and COPs

The water temperature in the network depends on several factors, including the actual flow rates, the heat transfer through the ground, and the location in the network. Fig. 10a shows the supply water temperature, the return water temperature and the ground temperature calculated by the annual simulation performed by the model. The supply and return water temperatures are evaluated as the temperature leaving and entering the central plant node, respectively. The supply temperature is constant at 15 °C all year round, as it is assumed that the plant is an unlimited source of energy at 15 °C. The return water temperature varies between 7 and 19 °C. In winter, the return temperature is lower than the supply temperature, indicating a prevalence of heating demand. The average network temperature is higher than the ground temperature, causing heat transfer from the network to the ground, which is considered a heat loss. In summer, the network has a prevalent cooling demand, as the return temperature is higher than the supply temperature. The ground temperature is mostly higher than the network temperature. Therefore, heat transfers from the ground to the network, which is not desired during times of cooling. Note that, for graphical readability, only the return water temperature profile of the case LT-F is plotted in Fig. 10a. It is interesting to note that the maximum difference between the return temperature of the four cases is 0.2 K.

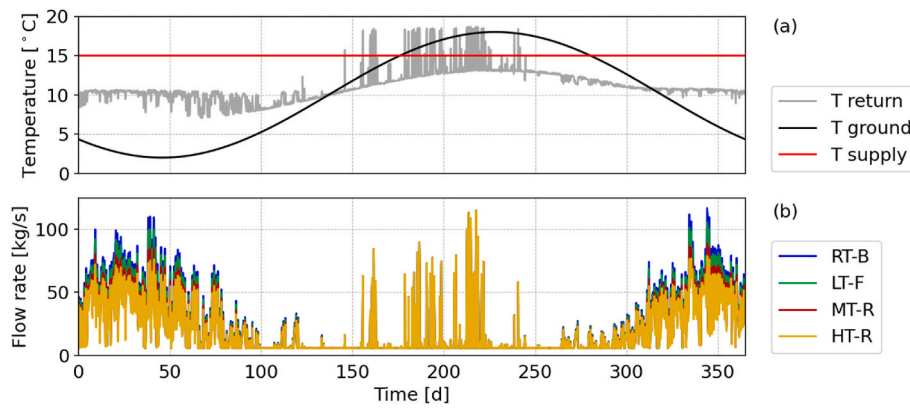


Fig. 10. Supply, return and ground temperature in the network (a), mass flow rate flowing through the central plant (b).

Fig. 10b shows the flow rate through the central plant for the four cases. In winter, it is noticed that the lower the heat distribution temperatures in the buildings, the higher is the required mass flow rate in the network. This is due to the fact that low temperatures in the heat distribution building system lead to high COP of the heat pump, which causes the removal of a higher amount of heat at the evaporator (network side).

This aspect can be described in more detail using the p-h diagram of a refrigerant under different operating conditions, as shown in Fig. 11. While assuming a constant heat exchange at the condenser ( $h_3-h_4 = h_3'-h_4'$ ), a reduction of the heat distribution temperature (temperature at the condenser) leads to a higher heat exchange at the evaporator ( $h_2-h_1 > h_2'-h_1'$ ). Since the temperature difference between inlet and outlet is fixed at 4 K, the network is required to deliver a higher mass flow rate to satisfy the heating demand. In summer, there is no difference between the four cases, as only the heat pumps for DHW operate.

Table 4 shows the seasonal COP values of the heat pumps for space heating along the five clusters. As expected, the highest COPs are obtained for the RT-B case, where they vary between 9.12 (Cluster A) and 8.68 (Cluster E). The HT-R case presents the lowest COPs, which vary between 3.13 (Cluster A) and 3.04 (Cluster E). The small differences in the COP values along the network (i.e., among the different clusters) are due to heat transfer between the fluid and the ground, which mostly affects Cluster E, as this is the farthest substation from the central plant. The decrease of the COP from Cluster A to Cluster E illustrates the above mentioned effect: the heat transfer from the network to the ground in winter is a loss and decreases the energy efficiency.

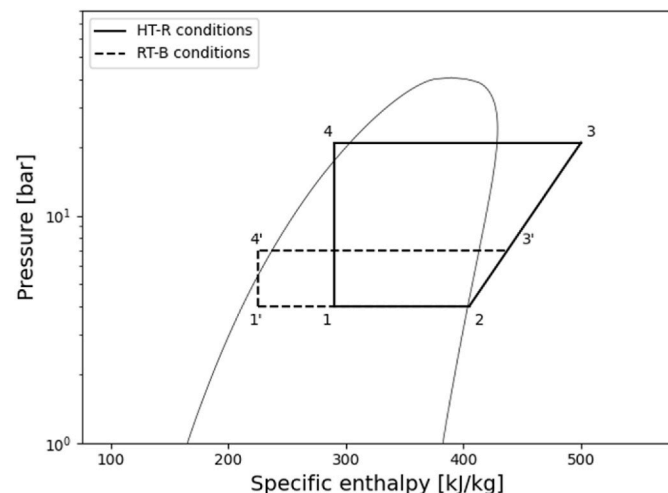


Fig. 11. P-h diagram of heat pump cycle.

Table 4

Seasonal COP values for the four cases in correspondence of the five building clusters.

	Cluster A	Cluster B	Cluster C	Cluster D	Cluster E
RT-B	9.12	9.01	8.92	8.77	8.68
LT-F	5.99	5.9	5.86	5.8	5.76
MT-R	3.9	3.86	3.82	3.8	3.77
HT-R	3.13	3.08	3.07	3.06	3.04

### 3.2. Electricity use of heat pumps and circulation pumps

The main evaluation indicator for the comparison of the energy performance among the four cases is the electric annual energy use of the heat pumps and the circulation pumps (Fig. 12a).

The annual electric energy used by the heat pumps (normalized by the total floor area) is 10.4 kWh/m<sup>2</sup> in the HT-R case, 9.2 kWh/m<sup>2</sup> in the MT-R case, 7.5 kWh/m<sup>2</sup> in the LT-F case, and 6.2 kWh/m<sup>2</sup> GWh in the RT-B case. Reducing the distribution temperatures of the building heating system from 70 °C (HT-R) to 23 °C (RT-B) leads to around 40% annual electric energy savings for the operation of the heat pumps.

The annual electric energy used by the circulation pump is 0.16 kWh/m<sup>2</sup> in the HT-R case, 0.2 kWh/m<sup>2</sup> in the MT-R case, 0.26 kWh/m<sup>2</sup> in the LT-F case and 0.3 kWh/m<sup>2</sup> in the RT-B case. The circulation pump energy use is thus between 1% and 5% of the total electric energy use. This is in agreement with the 2.5% found in the case study for the ground-water-based thermal network in Ref. [28]. In relation to the total thermal energy demand (4.36 GWh/y), the circulation pump electric energy use is between 0.5% and 0.8%.

The results indicate that using heat distribution temperatures of 23 °C leads to electric energy use for the circulation pump that is almost double compared to the HT-R case. This behaviour reflects the findings illustrated in Fig. 10b, where it is shown that low heat distribution temperatures in the building system – and hence low temperature lifts over the heat pump – lead to high mass flow rates in the network. The reason for this effect is that exergy required, i.e., electricity for the compressor, is lower the smaller the temperature lift. In summary, to provide equal energy at the condenser, more energy is required from the evaporator if the temperature lift is low.

Globally, the total annual electric energy use for heating and cooling is 10.6 kWh/m<sup>2</sup> in the HT-R case, 9.4 kWh/m<sup>2</sup> in the MT-R, 7.8 kWh/m<sup>2</sup> in the LT-F case, and 6.5 kWh/m<sup>2</sup> in the RT-B case. Electric energy savings of around 39% were obtained for the RT-B case in comparison to the HT-R case.

The seasonal dynamic variation of the electric energy use for heat pumps is illustrated in Fig. 12b. As expected, the results show a pattern with large electric energy use in winter, represented by a steep slope of the curves. In summer, the curves illustrate a smoother slope, as the heat

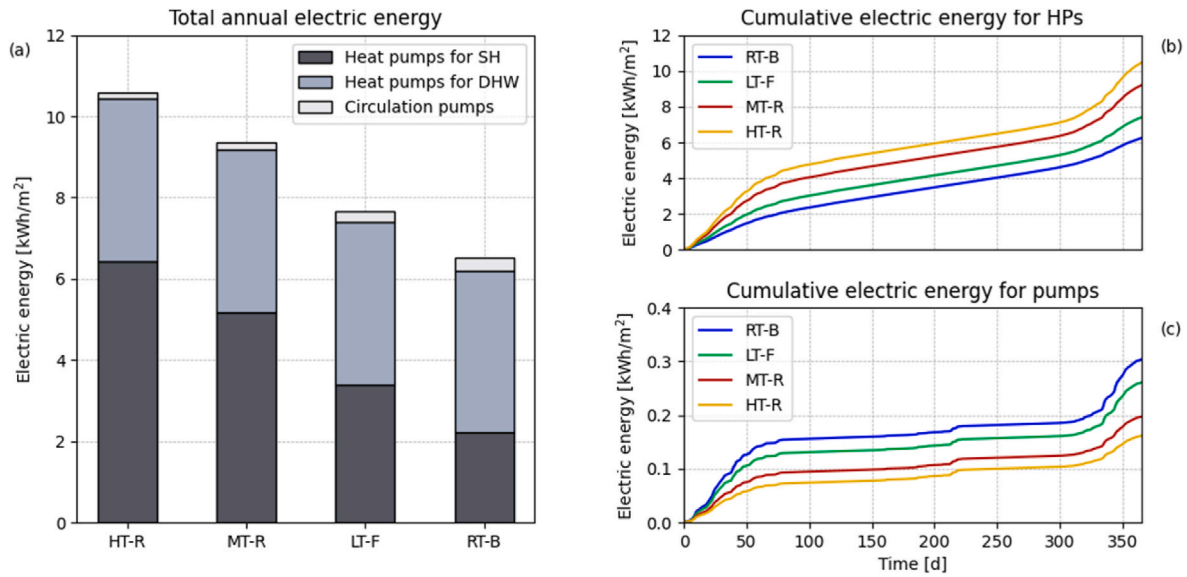


**Fig. 12.** Electric energy use (values are normalized by the total floor area). a) Annual electric energy use for heat pumps and circulation pumps. b) Cumulative electric energy use for heat pumps. Note that the cumulative energy use profile of DHW is equal in all four cases. c) Cumulative energy use for circulation pumps.

pumps for space heating are not operating.

Fig. 12c shows the dynamic variation of the electric energy use for the circulation pumps. Similarly, large electric energy use is noticed during winter. As the cold season ends, the curves show a gradual slope, indicating that the network circulates water only for domestic hot water and cooling.

#### 4. Limitations

Limitations of this study mainly refer to the modeling assumptions. A constant domestic hot water profile was considered for all building typologies. This assumption neglects the daily peaks in single consumers. The average and constant demand over the entire network considers the large variety of users' behaviour in utilizing domestic hot water, hence smoothening the load profile of DHW.

Regarding space heating demand, uniform assumptions of user behaviour were made. In reality, inhabitants will set different room temperature set-points, ventilation schemes, etc.

The central plant was considered as an unlimited source of heat/cold, which can cover the entire heating and cooling demands in the network and impose a constant supply water temperature of 15 °C. In reality, central plants are limited in size, and the supply water temperature in 5GDHC networks is typically floating around a design value.

Another limitation refers to the ground modeling. Even though the ground surrounding the pipes was modelled in more detail than in other studies, as the thermal inertia was considered by using dynamic heat conduction and storage with a finite difference approach, a more complex modeling approach may be required to accurately analyze the heat exchange between the pipes and the ground.

Finally, thermal loads for space heating, domestic hot water and space cooling were included in the model as time series. This is a common approach in district energy simulation studies, but decoupling the network from the buildings implies that the bidirectional dynamic interaction between supply and demand is ignored.

#### 5. Discussion

##### 5.1. Pipe sizing

Circulation pump energy is highly sensitive to the diameter of the piping network. By using larger pipe diameters than the design values,

the circulation pump energy can be reduced. However, increasing the diameter also increases the costs, consisting of piping, trenching and installation. Typically, in conventional district heating networks (i.e. not equipped with heat pumps in the substations) the pipe diameters are designed starting from the peak heating demand of the buildings in each piping branch. In 5GDHC systems, this heating demand is represented by the condenser heat flow rate, which, however, may not be used for pipe sizing. The relevant design parameter in 5GDHC systems is in fact the evaporator heat flow rate of the substation's heat pumps, which depends on the COP. This means that a proper pipe sizing design of 5GDHC systems should take into consideration which heat distribution systems are installed in the buildings, and which COPs are achieved by the heat pumps at design temperature lifts. However, this information may not be available at the early design stages, and therefore, average COP values may need to be used. In the present study, as mentioned in section 2.3.4, a default COP value of 3 was considered in all four cases.

If details about heat pumps operation are available, the design load of the distribution network in each pipe segment  $i$  may be calculated as

$$\dot{Q}_{des,load,i} = \dot{Q}_{DHW,i} \left( 1 - \frac{1}{COP_{HP,DHW}} \right) + \max \left[ \dot{Q}_{SH,i} \left( 1 - \frac{1}{COP_{HP,SH}} \right), \dot{Q}_{SC,i} \right] \quad (5)$$

where  $\dot{Q}_{SH,i}$  is the design load for space heating in pipe segment  $i$ ,  $\dot{Q}_{DHW,i}$  is the design load for domestic hot water in pipe segment  $i$ ,  $\dot{Q}_{SC,i}$  is the design load for space cooling,  $COP_{HP,SH}$  is the design COP of heat pumps for space heating and  $COP_{HP,DHW}$  is the design COP of heat pumps for DHW. Equation (5) assumes that the design load for domestic hot water is equal in winter and summer, and that the design loads for space heating and space cooling do not coincide in time. To reduce first costs, the design load should consider diversity, and it may not be at peak condition but rather at some annual cumulative frequency of occurrence [49].

Table 5 shows the pipe dimensions when applying this design methodology to the Kjøge Nord case study. The use of low heat distribution temperatures in buildings require larger pipe diameters to keep the pressure drops in the circuit within the design values. On the other hand, smaller pipes are typically sufficient when buildings are equipped with high-temperature heat distribution systems. Note that the pipe diameter of the segment Plant-A is equal for all four cases. This is due to the fact that the design load in this segment is done with respect to the

**Table 5**

Pipe segment diameter [m]. The column “default” shows the pipe diameters used for the simulations previously presented, where the pipe dimensions were kept constant among the four cases.

	Default (COP = 3)	RT-B	LT-F	MT-R	HT-R
Plant - A	0.24	0.24	0.24	0.24	0.24
A-B	0.19	0.2	0.18	0.18	0.17
B-C	0.17	0.19	0.18	0.17	0.16
C-D	0.15	0.17	0.16	0.15	0.14
D-E	0.13	0.14	0.14	0.12	0.12

cooling demand.

5.2. Generalizability of findings

In this paper, the influence of heat distribution temperatures on the energy performance of 5GDHC systems was carried out for a specific case study located in Denmark using detailed dynamic models in Modelica. To extend the results obtained from this analysis to other cases, a simplified one-equation mathematical model is proposed. The model concept is based on a lumped parameter approach where all network users are considered as a single aggregated annual load. Under steady-state conditions, the annual electric energy use for space heating in a 5GDHC system as shown in Fig. 5 can be calculated as

$$E_{el,HP} = \frac{Q_{SH}}{COP_{avg,SH}}, \tag{6}$$

where  $Q_{SH}$  is the annual heating demand for space heating and,  $COP_{avg,SH}$  is the average COP of heat pumps. By substituting equation (1) into equation (6):

$$E_{el,HP} = Q_{SH} \left( \frac{1}{\eta} - \frac{T_{eva}}{\eta \cdot T_{con,SH}} \right), \tag{7}$$

where  $\eta$  is the Carnot effectiveness of the heat pumps,  $T_{eva}$  is the evaporation temperature and  $T_{con,SH}$  is the temperature at the condenser of the heat pump for space heating. The values of condenser and evaporator temperatures should take into consideration pinch temperatures.

The electric energy savings achievable by lowering the temperature in the heat distribution systems can be calculated and directly visualized by considering equation (7) with  $T_{con,SH}$  as the independent variable, and comparing it with the reference case of a 5GDHC system that has a space heating distribution temperature of 70 °C, as follows

$$S_{el,HP} = 100 \left( 1 - \frac{\left( 1 - \frac{T_{eva}}{T_{con,SH}} \right)}{\left( 1 - \frac{T_{eva}}{273.15+72} \right)} \right), \tag{8}$$

Fig. 13 illustrates the function represented by equation (8) for a typical case with source temperature  $T_{eva} = 9$  °C. Note that an evaporator temperature of 9 °C corresponds to 15 °C distribution network temperature and 4 K temperature difference over the evaporator with 2 K of pinch temperature.

An interesting aspect is that, despite the function having a hyperbolic form, in the region of interest it assumes a nearly linear behaviour. This trend enables to draw a linear function as:

$$S_{el,HP} = -1.53 \cdot T_{con,SH} + 108 \tag{9}$$

which shows that about 1.5% of electric energy savings can be achieved for each temperature degree reduction in the heat distribution system.

Fig. 13 and equation (9) show electric energy savings compared to a 70 °C design temperature. However, for low-temperature heating systems, the sensitivity is higher. If the 72 °C condenser temperature in (8) were to be replaced by a 37 °C condenser temperature, then each deviation by 1 K leads to a change in electricity consumption of 3%. Thus,

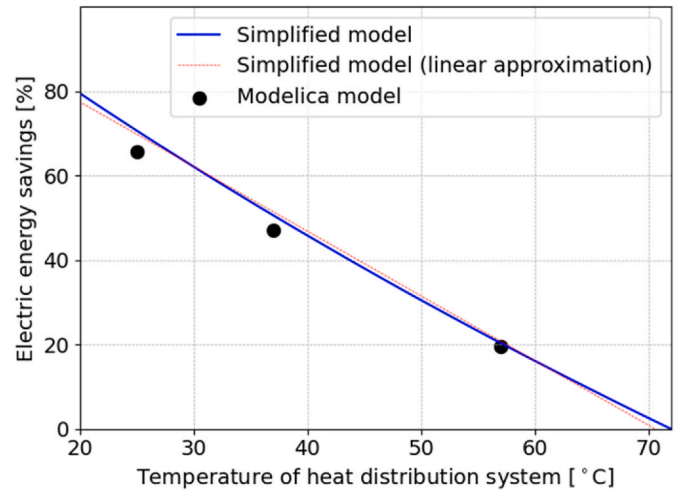


Fig. 13. Electric energy savings as a function of heat distribution temperature.

this highlights the critical importance of proper design, thermal integration, and control of low-temperature heat pump systems.

In view of this sensitivity, it is remarkable that many jurisdictions have ambitious plans to deploy heat pumps, yet they lack energy codes or other strategies that keep their heating supply temperature low in the future. For example, in Denmark, heating supply temperatures are not regulated in the building code [50]. In California, the building energy standard only regulates maximum return temperature, but has no regulation regarding the supply temperature [51] and US states generally have no regulations regarding the supply or return water temperatures. In Switzerland, supply temperatures are regulated in the *Mustervorschriften der Kantone im Energiebereich (MuKEN)* [52], and discussed in Refs. [53,54].

Fig. 13 also depicts the values obtained with Modelica models. It is noticed that the total annual electric energy savings can be predicted with quite a good accuracy by the simplified model, especially for systems with high heat distribution temperatures. Such simple analyses could be useful for early-stage design of 5GDHC systems, where rough estimations and comparisons among different design scenarios are of interest.

Nevertheless, detailed energy modeling and simulation techniques become necessary in advanced stages of the design process, where local values of operating parameters need to be calculated and carefully analyzed, or if the risk of using the simplified method is too high in view of the design and associated investment decisions. For example, in 5GDHC systems, a critical operating parameter is the water temperature

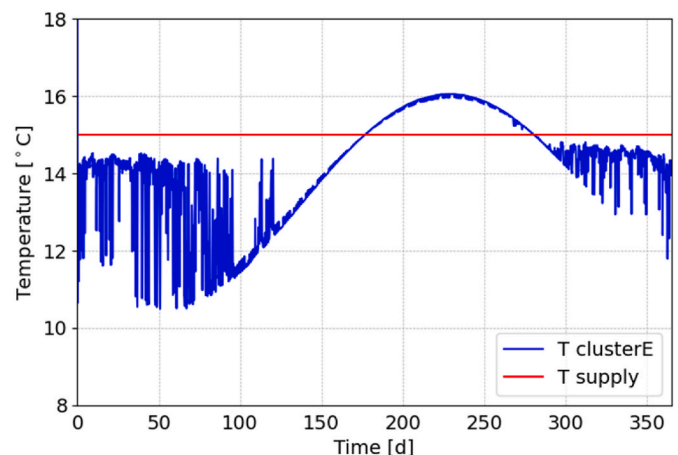


Fig. 14. Water temperature entering the substation in cluster E (case LT-F).

entering the substation, which must be lower than a certain value in order to enable direct cooling (i.e. via a heat exchanger). As shown in Fig. 14, in summer, the water temperature entering the substation of Cluster E is at 16 °C, which is higher than the water temperature supplied by the plant. This is due to heat transfer with the ground. In the specific case of Køge Nord, no cooling was needed in Cluster E, but in other cases, depending on the specific cooling system installed in the building, such temperature may not be sufficient for compressor-less cooling.

## 6. Conclusions

In this article, the energy performance and sizing criteria of 5GDHC networks were analyzed as a function of the heat distribution temperature in the building systems connected to the district network. A 5GDHC energy simulation model was developed in Modelica, and electric energy consumptions were calculated for four different building heating systems, with temperatures varying between 70 °C and 23 °C. Simulations were carried out for a case study located in Denmark.

Results showed that the use of low heat distribution temperatures in building systems has two opposite effects on the electric energy consumption of 5GDHC systems. On the one hand, decentralized heat pumps operate with higher COPs, with a consequent reduction of the electric energy consumption for the compressors. On the other hand, a higher amount of heat flow rate is required by the heat pump evaporator, leading to higher water mass flow rates in the network, with a consequent increase in electric energy consumption for the circulation pumps.

Globally, since the electric energy consumption for circulation pumps represents a small fraction of the total energy consumption, the overall effect results in a reduction of electric energy consumption. In particular, using heat distribution temperatures in building systems of 23 °C leads to around 39% annual total electric energy savings compared to the case with heat distribution temperatures of 70 °C.

In terms of sizing, the higher water mass flow rates required for building systems with low heat distribution temperatures suggest using larger pipes to keep the pressure drop within the same design values.

The paper also proposed a simplified one-equation model to estimate the electric energy savings achievable by lowering the temperature in the building heating systems connected to 5GDHC networks. It is found that each temperature degree reduction in the heat distribution system leads to about 1.5% electric energy savings in comparison to the reference case at 70 °C. If the reference temperature is 35 °C, then 3% electric savings would be achieved with every K reduction in heating supply temperature.

In conclusion, this work highlights the importance of a holistic system design for the 5GDHC technology, where building heat distribution systems and district network are intertwined and affect each other's operation and performance.

## Credit author statement

**Alessandro Maccarini:** Conceptualization, Methodology, Software, Formal analysis, Investigation, Data curation, Writing – original draft, Visualization. **Artem Sotnikov:** Methodology, Software, Formal analysis, Writing – review & editing. **Tobias Sommer:** Conceptualization, Methodology, Writing – review & editing. **Michael Wetter:** Conceptualization, Software, Writing – review & editing. **Matthias Sulzer:** Conceptualization, Methodology, Writing – review & editing. **Alireza Afshari:** Project administration, Funding acquisition.

## Declaration of competing interest

The authors declare that they have no known competing financial interests or personal relationships that could have appeared to influence the work reported in this paper.

## Data availability

Data will be made available on request.

## Acknowledgments

This work was supported by the Danish Energy Agency, under the Energy Technology Development and Demonstration Program (EUDP), journal no. 64019-0548.

This research was supported by the Assistant Secretary for Energy Efficiency and Renewable Energy, Building Technologies Office, of the U.S. Department of Energy, under Contract No. DE-AC02-05CH11231.

This work was supported by the SWEET program “Decarbonization of Cooling and Heating in Switzerland” of the Swiss Federal Office of Energy (SFOE), Contract No. Si/502260-01.

This work emerged from the IBPSA Project 1, an international project conducted under the umbrella of the International Building Performance Simulation Association (IBPSA). Project 1 will develop and demonstrate a BIM/GIS and Modelica framework for building and community energy system design and operation.

## References

- [1] United Nations, Department of Economic, Affairs Social, Division Population. *World urbanization prospects: the 2018 revision*. New York: United Nations; 2019. ST/ESA/SER.A/420.
- [2] Lund H, Werner S, Wiltshire R, Svendsen S, Thorsen JE, Hvelplund F, Vad Mathiesen B. 4th Generation District Heating (4GDH): integrating smart thermal grids into future sustainable energy systems. *Energy* 2014;68:1–11. <https://doi.org/10.1016/j.energy.2014.02.089>.
- [3] Sorknaes P, Østergaard PA, Thellufsen JZ, Lund H, Nielsen S, Djørup S, Sperling K. The benefits of 4th generation district heating in a 100% renewable energy system. *Energy* 2020;213:119030. <https://doi.org/10.1016/j.energy.2020.119030>.
- [4] Averfalk H, Werner S. Economic benefits of fourth generation district heating. *Energy* 2020;193:116727. <https://doi.org/10.1016/j.energy.2019.116727>.
- [5] International Energy Agency (IEA). *The future of cooling - opportunities for energy-efficient air conditioning*. Paris: IEA; 2018.
- [6] Buffa S, Cozzini M, D'Antoni M, Baratieri M, Fedrizzi R. 5th generation district heating and cooling systems: a review of existing cases in Europe. *Renew Sustain Energy Rev* 2019;104:504–22. <https://doi.org/10.1016/j.rser.2018.12.059>.
- [7] Boesten S, Ivens W, Dekker SC, Eijdens H. 5th generation district heating and cooling systems as a solution for renewable urban thermal energy supply. *Adv Geosci* 2019;49:129–36. <https://adgeo.copernicus.org/articles/49/129/2019/>.
- [8] Revesz A, Jones P, Dunham C, Davies G, Marques C, Matabuena R, Scott J, Maidment G. Developing novel 5th generation district energy networks. *Energy* 2020;201:117389. <https://doi.org/10.1016/j.energy.2020.117389>.
- [9] Sulzer M, Werner S, Mennel S, Wetter M. Vocabulary for the fourth generation of district heating and cooling. *Smart Energy* 2021;1:100003. <https://doi.org/10.1016/j.SEGY.2021.100003>.
- [10] Lund H, Østergaard PA, Nielsen TB, Werner S, Thorsen JE, Gudmundsson O, Arabkoosar A. Perspectives on fourth and fifth generation district heating. *Energy* 2021;227:120520. <https://doi.org/10.1016/j.energy.2021.120520>.
- [11] Pellegrini M, Bianchini A. The innovative concept of cold district heating networks: a literature review. *Energies* 2018;11:236. <https://doi.org/10.3390/en11010236>.
- [12] Bünning F, Wetter M, Fuchs M, Müller D. Bidirectional low temperature district energy systems with agent-based control: performance comparison and operation optimization. *Appl Energy* 2018;209:502–15. <https://doi.org/10.1016/j.apenergy.2017.10.072>.
- [13] Sulzer M. *Effizienzsteigerung mit Anergienetzen: potenziale-Konzepte-Beispiele*. Tech rep. INRETIS - Energie und Gebäudetechnik 2011.
- [14] Calixto S, Cozzini M, Manzolini G. Modelling of an existing neutral temperature district heating network: detailed and approximate approaches. *Energies* 2021;14:379. <https://doi.org/10.3390/en14020379>.
- [15] Wirtz M, Kivillip L, Remmen P, Müller D. Quantifying demand balancing in bidirectional low temperature networks. *Energy Build* 2020;224:110245. <https://doi.org/10.1016/j.enbuild.2020.110245>.
- [16] Prasanna A, Dorer V, Vetterli N. Optimisation of a district energy system with a low temperature network. *Energy* 2017;137. <https://doi.org/10.1016/j.energy.2017.03.137>.
- [17] Vetterli N, Sulzer M, Up Menti. Energy monitoring of a low temperature heating and cooling district network. Lausanne, Switzerland: CISBAT 2017 Conference; 2017. p. 6–8 [September].
- [18] Schluck T, Krauchi P, Sulzer M. Non-linear thermal networks - how can a meshed network improve energy efficiency? CISBAT 2015 Conference. 2015–11 September. Lausanne, Switzerland.
- [19] Franzén I, Nedar L, Andersson M. Environmental comparison of energy solutions for heating and cooling. *Sustainability* 2019;11:7051. <https://doi.org/10.3390/su11247051>.

- [20] Wirtz M, Kivillip L, Remmen P, Müller D. 5th Generation District Heating: a novel design approach based on mathematical optimization. *Appl Energy* 2020;260:114158. <https://doi.org/10.1016/j.apenergy.2019.114158>.
- [21] Zarin Pass R, Wetter M, Piette MA. A thermodynamic analysis of a novel bidirectional district heating and cooling network. *Energy* 2018;144:20–30. <https://doi.org/10.1016/j.energy.2017.11.122>.
- [22] Wetter M, Hu J. Quayside energy systems analysis. Lawrence Berkeley National Laboratory; 2019. LBNL-2001197, <https://escholarship.org/uc/item/957066mw>.
- [23] Sulzer M, Sotnikov A, Sommer T. Reservoir-Niedertemperatur Netztopologie für die Vermaschung von thermischen Netzen. In: Status-Seminar Forschen für den Bau im Kontext von Energie und Umwelt. Switzerland: Zürich; 2018.
- [24] Sommer T, Sulzer M, Wetter M, Sotnikov A, Mennel S, Stettler C. The reservoir network: a new network topology for district heating and cooling. *Energy* 2020;117418. <https://doi.org/10.1016/j.energy.2020.117418>. 199, 2020.
- [25] Von Rhein J, Henze GP, Long N, Fu Y. Development of a topology analysis tool for fifth generation district heating and cooling networks. *Energy Convers Manag* 2019;196:705–16. <https://doi.org/10.1016/j.enconman.2019.05.066>.
- [26] Wirtz M. nPro: a web-based planning tool for designing district energy systems and thermal networks. *Energy* 2023;268:126575. <https://doi.org/10.1016/j.energy.2022.126575>.
- [27] Wirtz M, Neumaier L, Remmen P, Müller D. Temperature control in 5th generation district heating and cooling networks: an MILP-based operation optimization. *Appl Energy* 2021;288:116608. <https://doi.org/10.1016/j.apenergy.2021.116608>.
- [28] Sommer T, Sotnikov A, Sulzer M, Scholz V, Mischler S, Rismanchi B, Gjoka K, Mennel S. Hydrothermal challenges in low-temperature networks with distributed heat pumps. *Energy* 2022;257:124527. <https://doi.org/10.1016/j.energy.2022.124527>.
- [29] Edtmayer H, Nageler P, Heimrath R, Mach T, Hochenauer C. Investigation on sector coupling potentials of a 5th generation district heating and cooling network. *Energy* 2021;230:120836.
- [30] Abugabbara M, Javed S, Johansson D. A simulation model for the design and analysis of district systems with simultaneous heating and cooling demands. *Energy* 2022;261:125245. <https://doi.org/10.1016/j.energy.2022.125245>. Part A.
- [31] Quirosa G, Torres M, Chacartegui R. Analysis of the integration of photovoltaic excess into a 5th generation district heating and cooling system for network energy storage. *Energy* 2022;239:122202. <https://doi.org/10.1016/j.energy.2021.122202>.
- [32] Gonçalves P, Gaspar AR, Gameiro da Silva M. Comparative energy and exergy performance of heating options in buildings under different climatic conditions. *Energy Build* 2013;61:288–97.
- [33] Kazanci OB, Shukuya M, Olesen BW. Exergy performance of different space heating systems: a theoretical study, vol. 99. *Building and Environment*; 2016. p. 119–29.
- [34] Kerdan IG, Raslan R, Ruyssevelt P. An exergy-based multi-objective optimisation model for energy retrofit strategies in non-domestic buildings. *Energy* 2016;117:506–22.
- [35] Statistics Denmark. <https://www.dst.dk>. [Accessed 19 September 2022]. Accessed.
- [36] Maccarini A, Mans M, Sørensen CG, Afshari A. Towards an automated generator of urban building energy loads from 3D building models. In: Proceedings of the 14th Modelica conference. Sweden: Linköping; 2021. <https://doi.org/10.3384/ecp21181659>. September 20–24.
- [37] International Standard Organization. ISO 13790:2008 Energy performance of buildings — calculation of energy use for space heating and cooling. 2008.
- [38] Coskun C, Ertürk M, Oktay Z, Hepbasli A. A new approach to determine the outdoor temperature distributions for building energy calculations. *Energy Convers Manag* 2014;78:165–72.
- [39] Hangartner D, Ködel J, Mennel S, Sulzer M. Grundlagen und Erläuterungen zu Thermischen Netzen. March, 1–37, <https://www.energieschweiz.ch/home.aspx?p=22949,22963,22985>; 2018.
- [40] Maccarini A, Wetter M, Afshari A, Hultmark G, Bergsøe NC, Vorre A. Energy saving potential of a two-pipe system for simultaneous heating and cooling of office buildings. *Energy Build* 2017;134:234–47. <https://doi.org/10.1016/j.enbuild.2016.10.051>.
- [41] Maccarini A, Hultmark G, Afshari A, Bergsøe NC, Vorre A. Transferring heat among building zones through a room-temperature water loop—influence of climate and occupancy level. *Build Simulat* 2017;10:697–710. <https://doi.org/10.1007/s12273-017-0358-z>.
- [42] Maccarini A, Hultmark G, Bergsøe NC, Rupnik K, Afshari A. Field study of a self-regulating active beam system for simultaneous heating and cooling of office buildings. *Energy Build* 2020;224:110223. <https://doi.org/10.1016/j.enbuild.2020.110223>.
- [43] Mattsson SE, Elmqvist H, Otter M. Physical system modeling with Modelica. *Control Eng Pract* 1998;6(4):501–10. [https://doi.org/10.1016/S0967-0661\(98\)00047-1](https://doi.org/10.1016/S0967-0661(98)00047-1).
- [44] Kauko H, Kvalsvik KH, Rohde D, Nord N, Utne Å. Dynamic modeling of local district heating grids with prosumers: a case study for Norway. *Energy* 2018;151:261–71. <https://doi.org/10.1016/j.energy.2018.03.033>.
- [45] Saelens D, De Jaeger I, Bünning F, Mans M, Vandermeulen A, Van der Heijde B, Garreau E, Maccarini A, Ronneseth Ø, Sartori I, Helsen L. Towards a DESTEST: a district energy simulation test developed in IBPSA project 1. In: Proceedings of the 16th building simulation conference, rome, Italy; 2019. p. 2–4 [September].
- [46] Wetter M, Van Treeck C, Helsen L, Maccarini A, Saelens D, Robinson D, Schweiger G. IBPSA Project 1: BIM/GIS and Modelica framework for building and community energy system design and operation - ongoing developments, lessons learned and challenges. *IOP Conf Ser Earth Environ Sci* 2019;323:012114.
- [47] Wetter M, Zuo W, Nouidui TS, Pang X. Modelica buildings library. *Journal of Building Performance Simulation* 2014;7(4):253–70. <https://doi.org/10.1080/19401493.2013.765506>.
- [48] Eckert E, Drake RM. Heat and mass transfer. New York, NY, USA: McGraw-Hill Inc.; 1959.
- [49] Winter W, Haslauer T, Oberberger I. Untersuchungen der Gleichzeitigkeit in kleinen und mittleren Nahwärmenetzen, vol. 9. *Euroheat & Power*; 2001. 2001 und 10/2001.
- [50] BR18 Bygningsreglementet (. <https://byggningsreglementet.dk/>).
- [51] Title 24, Part 6. Building energy efficiency standards for residential and nonresidential buildings. Sacramento, CA: California Energy Commission; 2022.
- [52] Mustervorschriften der Kantone im Energiebereich (MuKEN). [https://www.endk.ch/de/ablage/grundhaltung-der-endk/MuKEN2014\\_d-2018-04-20.pdf/@download/file/MuKEN2014\\_d-%282018-04-20%29.pdf](https://www.endk.ch/de/ablage/grundhaltung-der-endk/MuKEN2014_d-2018-04-20.pdf/@download/file/MuKEN2014_d-%282018-04-20%29.pdf).
- [53] Sulzer M, Hangartner D. Kalte fernwärme (Anergienetze)-Grundlagen-/Thesenpapier. Switzerland: Lucerne University of Applied Science; 2014.
- [54] Hangartner D, Ködel J, Mennel S, Sulzer M. Grundlagen und Erläuterungen zu Thermischen Netzen. Switzerland: Lucerne University of Applied Science; 2018.